

# Evolution of Massive Blackhole Triples II — The effect of the BH triples dynamics on the structure of the galactic nuclear

Masaki Iwasawa<sup>1,2</sup>, Yoko Funato<sup>1</sup> and Junichiro Makino<sup>2</sup>

iwasawa@cfca.jp

## ABSTRACT

In this paper, we investigate the structures of galaxies which either have or have had three BHs using  $N$ -body simulations, and compare them with those of galaxies with binary BHs. We found that the cusp region of a galaxy which have (or had) triple BHs is significantly larger and less dense than that of a galaxy with binary BHs of the same mass. Moreover, the size of the cusp region depends strongly on the evolution history of triple BHs, while in the case of binary BHs, the size of the cusp is determined by the mass of the BHs. In galaxies which have (or had) three BHs, there is a region with significant radial velocity anisotropy, while such a region is not observed in galaxies with binary BH. These differences come from the fact that with triple BHs the energy deposit to the central region of the galaxy can be much larger due to multiple binary-single BH scatterings. Our result suggests that we can discriminate between galaxies which experienced triple BH interactions with those which did not, through the observable signatures such as the cusp size and velocity anisotropy.

*Subject headings:* black hole: physics — black hole: binary — galaxies: nuclei — galaxies: structure — stellar dynamics — Three-body problem:general — methods:  $n$ -body simulations

## 1. Introduction

According to recent observations, elliptical galaxies can be classified into two groups: “weak-cusp” galaxies and “strong-cusp” galaxies (Lauer et al. 1995; Faber et al. 1997). The

---

<sup>1</sup>Department of General System Studies, University of Tokyo, 3-8-1 at Komaba, Komaba, Meguro-ku, Tokyo 153-8902, Japan

<sup>2</sup>Division of Theoretical Astronomy, National Astronomical Observatory, 2-2-1 Osawa, Mitaka, Tokyo 181-8588, Japan

central surface brightness profiles of the weak-cusp galaxies are expressed as  $\Sigma(R) \propto R^{-\gamma}$  with  $\gamma \leq 0.3$ , and those of the strong-cusp galaxy the same formula with  $\gamma \geq 0.5$ . The slope of the volume density profile of strong-cusp galaxies is around  $-2$ , being consistent with the isothermal cusp. Such a steep cusp is naturally formed in dissipative process involving gas dynamics and star formation. On the other hand, the weak cusp corresponds to the slope of the volume density shallower than  $-1$ , which is not likely to be formed through dissipative process.

One possible way to form a weak cusp is the merging of two galaxies containing black holes (BHs). When two galaxies, each with a black hole, merge, two BHs sink toward the center of the merger remnant to form a binary through the dynamical friction (Begelman, Blandford, & Rees 1980). The back reaction of the dynamical friction heats up field stars. As a result, a shallow cusp of stars develops in the central region (Ebisuzaki et al. 1991; Nakano & Makino 1999; Merritt 2006).

One problem with this binary BH scenario is what would be the final fate of the binary BH. Begelman, Blandford, & Rees (1980) pointed out that the merging timescale of the binary BH might be very long, after the binary BH ejected out the stars which can interact with the binary (loss cone depletion). The stars will be supplied in the timescale of the relaxation time, which is much longer than the Hubble time. Recent  $N$ -body simulations confirmed this theoretical estimate (Makino & Funato 2004; Berczik, Merritt, & Spurzem 2005).

If galaxies are formed through hierarchical clusterings, in many cases, a binary BH is formed after a merger event. If there were sufficient gas left in the merger, interaction with gas might lead to the quick merging of the two BHs. However, in the case of “dry” mergers which would result in the formation of giant ellipticals, by definition not much gas is left and it would be difficult for two BHs to merge.

If one galaxy with binary BH and the other with single BH merge, the central BHs form a triple system. Iwasawa, Funato & Makino (2006, hereafter referred to as Paper I) investigated the evolution of triple BH system in the galactic center, using  $N$ -body simulations. They found that the strong binary-single BH interaction (Makino & Ebisuzaki 1994) and the Kozai cycle (Kozai 1962; Blas, Lee, & Socrates 2002) drives the eccentricity of the BH binary high enough that two BHs merge quickly through gravitational wave radiation. Hoffman & Loeb (2007) performed statistical simulations of evolution of central BH systems and reached a similar conclusion.

This paper is a follow-up of Paper I. In this paper, we investigate the structure of a galaxy containing three BHs. We also investigated their observational properties which

would help us to find galaxies which have (or had) triple BHs.

We performed  $N$ -body simulations of the evolution of triple (or binary) BH in a host galaxy, in order to study the dynamical evolution of the structure of stellar systems containing BHs. In our simulations, both dynamical evolution of BHs and that of field stars are integrated consistently. The interaction between BHs affects not only the evolution of themselves but also the spatial and kinematic structure of field stars around them. In turn, the distribution of field stars affects the interaction between BHs. To understand the structure of galaxies containing BHs, a self-consistent simulation in which the orbits of BHs and stars are treated self-consistently is essential.

The structure of this paper is as follows. In section 2, we describe the initial models and the method of our numerical simulations. In section 3, we show the effect of the BH triples dynamics on the structure of the galaxy. Summary and discussion are given in section 4.

## 2. Initial Models and Numerical Methods

### 2.1. Initial Models

The initial setup of the models is basically the same as that in Paper I. For the galaxy model, we used a King model with  $W_0 = 11$ , where  $W_0$  is the nondimensional central potential of King models (King 1966; Binney & Tremaine 1987). We adopted the standard  $N$ -body units (Heggie & Mathieu 1986), in which  $m_{gal} = 1.0$ ,  $E_{gal} = -0.25$ ,  $G = 1$ . Here,  $m_{gal}$  and  $E_{gal}$  are the total mass and total binding energy of the galaxy not including BHs and  $G$  is the gravitational constant. We placed three equal-mass BH particles in  $N$ -body models of a spherical galaxy. Two of three BHs particles are initially placed at the position  $(\pm 0.005, 0.0, 0.0)$  with velocity  $(0.0, \pm 0.15, 0.0)$ , and the third one is at the position  $(0.1, 0.0, 0.0)$  with velocity  $(0.0, 0.0, 0.0)$ . In order to compare the structure of a galaxy with three BHs with that of a galaxy with two BHs, we also performed simulations of galaxies with two BHs. Total mass of BHs in two-BH models was kept to be the same as that in the corresponding three-BH models. For two-BH model, two BHs are placed at the position  $(\pm 0.1, 0.0, 0.0)$  with velocity  $(0.0, \pm 0.1, 0.0)$ . The quantitative properties of models and initial conditions of our simulation is summarized in table 1.

We set the number of FS particles  $N_{FS} = 262144$  in all simulations. In order to investigate the effect of triple BHs on the galaxy, we set the mass ratio between galaxy and total mass of BHs to,  $m_{BH,tot}/m_{gal} \sim 0.003$ , where  $m_{BH,tot}$  is total mass of BH, in our standard model. This value is what is suggested by recent observations (Kormendy & Richstone 1995; Magorrian et al. 1998; Marconi & Hunt 2003). Table 2 shows all models.

## 2.2. Numerical Method

The numerical method is the same as that we used in Paper I. To summarize, we used a softened Newton gravity for the forces between field stars and those between each BH particle and field stars, while for forces between BH particles we applied post-Newtonian approximation to include the back reaction of gravitational radiation to the BHs. For the term corresponding to the radiation of the gravitational wave, we used approximately 2.5-order post-Newtonian approximation (Damour 1987).

We used the Plummer softening and set the value  $\epsilon_{\text{FS-FS}} = 10^{-4}$ ,  $\epsilon_{\text{FS-BH}} = 10^{-7}$  and  $\epsilon_{\text{BH-BH}} = 0.0$ , where  $\epsilon_{\text{XX-YY}}$  is softening parameters used for a XX particle - a YY particle interaction. Time integration scheme is the 4-th order Hermite scheme (Makino & Aarseth 1992) with individual variable time steps.

In order to calculate the acceleration due to field particles, we used GRAPE-6 (Makino et al. 2003), the special-purpose computer for the gravitational  $N$ -body problem. Forces from BH particles, both Newtonian and gravitational wave terms, are calculated on the host computer. In all runs, the energy (corrected for the loss of energy through GW radiation) is conserved better than 0.2 %

## 2.3. Physical Scales

The mass unit in our simulation corresponds to  $10^{11}M_{\odot}$ . Thus, the mass of each BH particle is  $10^8M_{\odot}$  in model M1T. We assume that the velocity dispersion of the initial King model at the King radius corresponds to 300 km/s. In other words, we set the light velocity  $c$  in the  $N$ -body unit to 1006. The unit of length and time are about 4.9kpc and 16Myr, respectively. The king radius is about 100pc.

## 3. Result

### 3.1. Evolution of BH System

Figure 1 shows the evolution of semi-major axis  $a$  and eccentricity  $e$  of BH binaries in all models. For models with triple BHs (model name MxT), the definition of the binary of BHs is the most strongly bound pair of three BHs. For the model M1T, jumps in  $a$  and  $e$  at  $T \sim 0.45, 0.96, 2.2, 3.7$  and  $4.8$  are results of interactions between the BH binary and the third BH. At  $T \sim 4.8$ , two BHs merged. This merging is driven by the impulsive

Table 1. Model Parameters

Parameter	Symbol	Value
Mass of galaxy	$m_{\text{gal}}$	1.0
Mass of FS	$m_{\text{FS}}$	1/262144
Mass of BH	$m_{\text{BH}}$	0.001 – 0.0045
Total mass of BHs	$m_{\text{BH,tot}}$	0.003 – 0.009
Number of FS	$N_{\text{FS}}$	262144
Number of BH	$N_{\text{BH}}$	2or3
Gravitational constant	$G$	1
Total energy	$E_{\text{gal}}$	–0.25
Softening between BHs	$\epsilon_{\text{BH-BH}}$	0.0
Softening between field stars and BH	$\epsilon_{\text{FS-BH}}$	$10^{-7}$
Softening between field stars	$\epsilon_{\text{FS-FS}}$	0.001

Table 2. Model List

Model name	$N_{\text{FS}}$	$N_{\text{BH}}$	$W_0$	$m_{\text{BH}}$	final state
M1T	262144	3	11	0.001	merge
M2T	262144	3	11	0.002	merge
M3T	262144	3	11	0.003	merge
M1B	262144	2	11	0.0015	no merge
M2B	262144	2	11	0.003	no merge
M3B	262144	2	11	0.0045	no merge

eccentricity growth caused by a binary-single interaction (Paper I), followed by the spiral-in due to gravitational wave radiation. The merging criterion we used here is that the distance between two BHs becomes smaller than three times of the Schwarzschild radius of a BH. We replaced the merged BHs by a new single BH. This new BH has the same mass, position and velocity as those of the barycenter of original binary.

As shown in Figure 1, the merged BH and the third one form a binary in model M1T. In models M1B and M1T, after  $T = 4.8$ ,  $a$  and  $e$  change slowly, and any BH merger does not occur until  $T = 10$ . In both models, a binary BH is left around the center of the host galaxy. Note that this slow shrink of the BH binary orbit is due to the refilling of the loss cone through two-body relaxation, which is enhanced because of the relatively small number of particles we used ( $N_{\text{FS}} = 262144$ ). In real galaxies the timescale of orbital evolution of binary BH would be much longer after the loss cone is depleted.

In model M2T, the overall behavior of BHs is rather similar to that in model M1T. After strong triple interactions at  $T = 0.35$  and  $2.2$ , the binary merged through gravitational wave radiation. On the other hand, in model M3T, after the first triple interaction at  $T = 0.3$ , the binary BH hardens through the interaction with field stars and finally merged through gravitational wave radiation. The difference between these three models is at least partly just a coincidence, since the final result depends on the outcome of the first triple encounter at time around  $0.4$ .

On the other hand, the behavior of models with binary BHs are all very similar, showing slow hardening driven by the loss-cone refill through two-body relaxation.

## 3.2. Density Structure

### 3.2.1. Density Profile

In Figure 2, we show the spatial (left) and surface (right) density profiles of models M3T and M3B at  $T = 3$  and  $T = 6$ . In both models the central density decreases and a weak cusp develops in the central region by  $T = 3$ . They do not change significantly after  $T = 3$ . This cusp is expressed as  $\rho \propto r^{-\gamma}$ , where  $\gamma \sim 0.5$ . For both models the slope of cusps can be explained by the simple theory of Nakano & Makino (1999).

From figure 2 we can see that there is a clear difference between models M1T and M1B. The size of the cusp region is bigger for M1T and the density is lower. This result indicates that a triple BH system is more efficient in heating the central region and ejecting the stars than a BH binary is.

In the case of a galaxy with a binary BH, a BH binary hardens in a monotonic fashion through interactions with FSs. In a galaxy with a triple BH system, a BH binary experiences multiple interactions with a single BH. In each event a single BH and the center of mass motion of binary BH acquires energy. This energy is then transferred to field stars through dynamical friction. As a result, the field stars are heated up and the cusp becomes wider. This mechanism is shown in Figure 3 more clearly.

### 3.2.2. Evolution of Cusp Region

In figures 3 and 4, time evolution of the Lagrangian radii of field stars, the cusp radius and radial positions of BHs for all models are plotted.

Following Casertano & Hut (1985), we defined the cusp radius as

$$r_{cusp} \equiv \frac{\sum_i \rho_i r_i}{\sum_i \rho_i}, \quad (1)$$

where  $\rho_i$  is the local mass density around the field particle with index  $i$  and the summation is done over field particles. The local mass density is defined as

$$\rho_i = \frac{m_{6,i}}{\frac{4}{3}\pi r_{6,i}^3}, \quad (2)$$

where,  $m_{6,i}$  is the total FS particle mass contained within  $r_{6,i}$  which is the distance from the field particle  $i$  to its sixth nearest neighbor.

In top panel of figure 3, the evolution of model M1T is shown. We can see that the Lagrangian radii and cusp radius change rather impulsively at the same time as the strong triple scattering events occur and BHs are ejected out of the central region. This expansion is because of the indirect heating due to the removal of massive BH particles from the center. After the scattering events, BHs sink towards the center of the system through dynamical friction, and the Lagrangian radii show small expansion. Thus, the expansion is driven by the BH particles. In the case of model M1B, the expansion is smooth and smaller than that in model M1T.

Figure 4 shows the evolution of the cusp radius and the mean cusp density of host galaxies for all models. We can clearly see that the expansion of the cusp radius in models MxT are driven by triple scattering events. In the case of model M3T, there was only one scattering event and therefore only one rapid expansion event for the cusp radius. In this model, the third BH is ejected out of the galaxy and never returned. Thus, one merged BH particle is left at the center of the galaxy. Slow decrease of the cusp radius is due to the thermal evolution of the field star system.

Figure 5 shows the density profile for all runs at  $T = 6$ . The density profile for all models are similar in their shapes. The density profile of model M3T is a bit steeper than those of other models. This is because only one binary-single scattering event is not enough to make the density profile  $\rho \propto r^{-0.5}$ .

For models with triple BHs (MxT), the radius and density of the cusp are determined not only by the total mass of BHs, but also by the number of binary-single BH scattering events. On the other hand, in the case of binary BHs, the total mass of BHs determines the structure of the cusp. In addition, in all cases the cusps in models MxT are bigger than those in models MxB of the corresponding BH mass.

### 3.3. Mass deficit

The discussion in the previous subsection can be re-interpreted in terms of the so-called “mass deficit” (Milosavljević & Merritt 2001, hereafter referred to as MM2001). They argued that one can estimate the mass removed by BH binary activity by comparing the singular isothermal profile and an actual cusp profile, and they argued that the difference, which they named “mass deficit”, retains the memory of the merging history of the black hole. Graham (2004) argued that MM2001’s method to estimate the mass deficit would give too large values like  $m_{\text{def}} \sim 10m_{\text{BH}}$ , where  $m_{\text{def}}$  is the mass deficit, while a more reasonable method would give  $m_{\text{def}} \sim m_{\text{BH}}$ . Merritt (2006) claimed that in repeated mergers  $m_{\text{def}} \sim Nm_{\text{BH}}$ , where  $N$  is the number of merging events, though his simulation result seems to suggest that such linear scaling does not hold for  $N > 3$ . In addition, simulations of the repeated merger of Merritt (2006) ignored the fact that additional BHs in reality comes with their host galaxies. Makino & Ebisuzaki (1996) have already shown that in the case of hierarchical repeated mergings, the density profile of merger remnant converge to a universal profile. In other words,  $m_{\text{def}}/m_{\text{BH}}$  does not tell much about the past merger history.

Figure 6 shows the ratio of mass deficit to total mass of BHs for all models. Here, we define the mass deficit as difference of mass at any given time with original mass within “break radius”, defined as the radius at which the initial profile and that at the current time intersect with each other (see Figure 2). In the case of binary BH runs (model MxB),  $m_{\text{def}}/m_{\text{BH,tot}}$  reaches about unity by  $T \sim 1$ , and the increase after that is due to loss-cone refilling by relaxation. Therefore, in the case where relaxation is negligible,  $m_{\text{def}} \sim m_{\text{BH,tot}}$ . In the case of triple BH system, however,  $m_{\text{def}}/m_{\text{BH,tot}}$  does tell about the past history of the evolution of the triple system. Thus, a galaxy with unusually large  $m_{\text{def}}/m_{\text{BH,tot}}$  is a good candidate for the host of triple BH.



In Figure 7, we compare the two methods to estimate the mass deficit, one of which is our definition and the other is used by MM2001. The estimate mass from MM2001 is systematically higher than real one. This difference is simply due to the fact that the method of MM2001 overestimates the initial mass with the break radius. We tried to use the method proposed by Graham (2004), but it turned out that the fit by a Sérsic profile is not appropriate for our galaxy model.

### 3.4. Velocity Structure

Figure 8 shows the velocity dispersion (top) and line-of-sight velocity (bottom) profiles at  $T = 6$ . In the central region, the velocity dispersion is increasing toward the center. Since the potential of BHs dominates the potential in the central region, the orbits of stars are almost Keplerian. The line-of-sight velocity dispersion shows the similar rise at the center.

In Figure 9, the velocity anisotropy for models M1T and M1B are compared. Here the anisotropy parameter is defined as

$$\beta \equiv 1 - \frac{\langle v_t^2 \rangle}{2\langle v_r^2 \rangle}, \quad (3)$$

where  $\langle v_t^2 \rangle$  and  $\langle v_r^2 \rangle$  are the tangential and radial mean square velocities. For model M1B, orbits are circular in the central region and  $\beta$  increases towards 0 as  $r$  increases at  $T = 3$  and 6. From figures 3 and 9, it is clear that, after two BHs settled and formed a binary in the center, the orbits of stars in the cusp becomes tangentially anisotropic and in the outer region the orbits remain isotropic. This is because the BH binary kicked out stars with radial orbits more efficiently than those with circular orbits in inner region.

For run M1T,  $\beta$  around the center is close to zero (isotropic) at  $T = 3$ , while that in outer region is positive. Thus, that stars are radially anisotropic around the outer edge of the central cusp, in the triple BH case. In this model,  $\beta$  around the center decreases after merging at  $T = 6$  like the two BH case. This is because of the slow evolution of the binary BH through the interaction with field stars.

## 4. DISCUSSION AND CONCLUSION

### 4.1. Possibility to Find Triple BH Systems

In previous sections, we have seen that the density and velocity structure of galaxies with triple BHs is different from that with two BHs. In Paper I, we showed that two of three

BHs in a galaxy merge within several dynamical times. The standard hierarchical clustering scenario of galaxy formation suggests that galaxies frequently merge and form ellipticals. Many elliptical galaxies, therefore, might host a binary BH. It is likely that many of them had a triple BH system once upon a time. Furthermore, there may be galaxies with a triple BH system. The lifetime of a triple BH system in a galaxy is several times the dynamical time of the core of the galaxy, which is about  $10^8$  years (100 M years). If we assume every elliptical galaxy have binary BH, and all large ellipticals are formed through mergings of elliptical galaxy. Speaking, 1% of large ellipticals could have triple BH systems now.

One possible way to discriminate between a galaxy with binary or single BH and that have (or had) triple BH is the measurement of the cusp radius and density. Our results suggest that the central cusp of a galaxy with three BHs is larger by a factor of few than that with binary BH. Thus the galaxy with a large cusp and low density in the central region might have (or had) three BHs.

Another possible way is to use the difference of velocity anisotropy. Anisotropy parameter of galaxy with three BHs is positive (radial) in the outer region due to the heating by BHs.

The anisotropy parameter  $\beta$  is estimated by the line of sight velocity and their higher moment, assuming that the galaxy is spherical. However, with this method it is difficult to obtain local anisotropy parameter in the central region of galaxies, unless the central density cusp is steep (Gerhard 1993). Another method is to fit the model with observational data (Cretton et al. 2000; Gebhardt et al. 2000, 2003). Figure 10 in Gebhardt et al. (2003) shows anisotropy profile of galaxies. The shapes of some galaxies profile in their paper, for example all “weak-cusp” galaxies (NGC3608, NGC4291, NGC4649), are similar to of our result in Figure 9. These galaxies might contain or have contained triple BHs.

## 4.2. Conclusions

In this paper, we investigated the effect of two- or three-BH systems on the structure of galaxies. We found that if the galaxy contains three BHs, (1) multiple three body scattering events reduce the density of the central cusp and increase the cusp radius and (2) in outer region, orbits of stars are likely to be radial. These difference allow us to discriminate the galaxies with two or three BHs.

We thank Toshiyuki Fukushige, Yusuke Tsukamoto and Keigo Nitadori for stimulating discussions and useful comments.

This research is partially supported by the Special Coordination Fund for Promoting Science and Technology (GRAPE-DR project), Ministry of Education, Culture, Sports, Science and Technology, Japan.

## REFERENCES

- Begelman, M. C., Blandford, R. D., & Rees, M. J. 1980, *Nature*, 287, 307
- Berczik, P., Merritt, D., & Spurzem, R. 2005, *ApJ*, 633, 680
- Binney, J., & Tremaine, S. 1987, *Galactic Dynamics* (Princeton: Princeton Univ. Press)
- Blas, O., Lee, M.H., & Socrates, A. 2002 *ApJ*, 578, 775
- Casertano, S., & Hut, P. 1985, *ApJ*, 298, 80
- Cretton, N., Rix, H.-W., & de Zeeuw, P. T. 2000, *ApJ*, 536, 319
- Damour, T. 1987, in *Three Hundred Years of Gravitation*, ed. S. Howking & W. Israel (Cambridge: Cambridge Univ. Press), 128
- Ebisuzaki, T., Makino, J., & Okumura, S. K. 1991, *Nature*, 354, 212
- Faber, S.M., et al. 1997, *AJ*, 114, 1771
- Gebhardt, K., et al. 2000, *AJ*, 119, 1157
- Gebhardt, K., et al. 2003, *ApJ*, 583, 92
- Gerhard, O. E. 1993, *MNRAS*, 265, 213
- Graham, A. W. 2004, *ApJ*, 613, L33
- Heggie, D. C., & Mathieu, R. D. 1986, in *The Use of Supercomputers in Stellar Dynamics*, ed. P. Hut & S. McMillan (Berlin: Springer), 233
- Hoffman, L., & Loeb, A. 2007, *MNRAS*, 377, 957
- Iwasawa, M., Funato, Y., & Makino, J. 2006, *ApJ*, 651, 1059
- King, I. R. 1966, *AJ*, 71, 276
- Kormendy, J., & Richstone, D. 1995, *ARA&A*, 33, 581

Kozai, Y. 1962, AJ, 67, 591

Lauer, T. R., et al. 1995, AJ, 110, 2622

Magorrian, J., et al. 1998, AJ, 115, 2285

Makino, J. & Aarseth, S. 1992, PASJ, 44, 141

Makino, J. & Ebisuzaki, T. 1994, ApJ, 436, 607

—. 1996, ApJ, 465, 527

Makino, J. & Funato, Y. 2004, ApJ, 602, 93

Makino, J., Fukushige, T., Koga, M. & Namura, K., 2003, PASJ, 55, 1163

Marconi, A., & Hunt, L. K. 2003, ApJ, 589, 21

Merritt, D. 2006, ApJ, 648, 976

Milosavljević, M., & Merritt, D. 2001, ApJ, 563, 34

Nakano, T. & Makino, J. 1999, ApJ, 510, 155

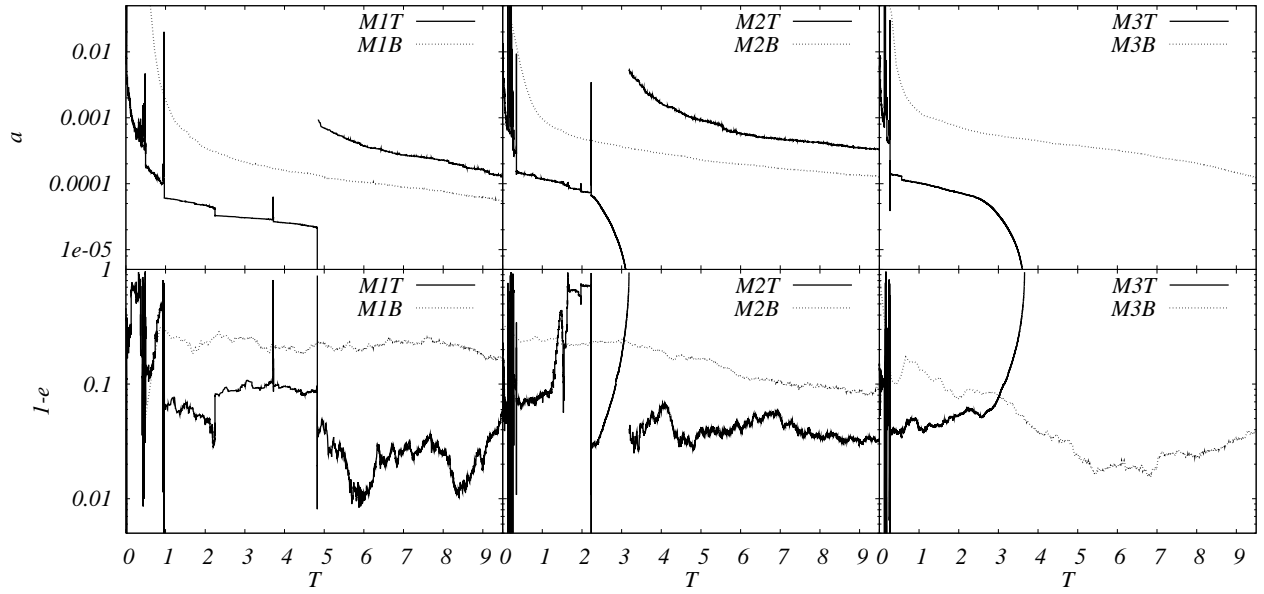


Fig. 1.— Evolution of semi-major axis (top) and eccentricity (bottom) of the most strongly bound pair of BHs for all models. Solid and dotted curves indicate the results of models MxT (triple BH) and MxB (binary BH) respectively.

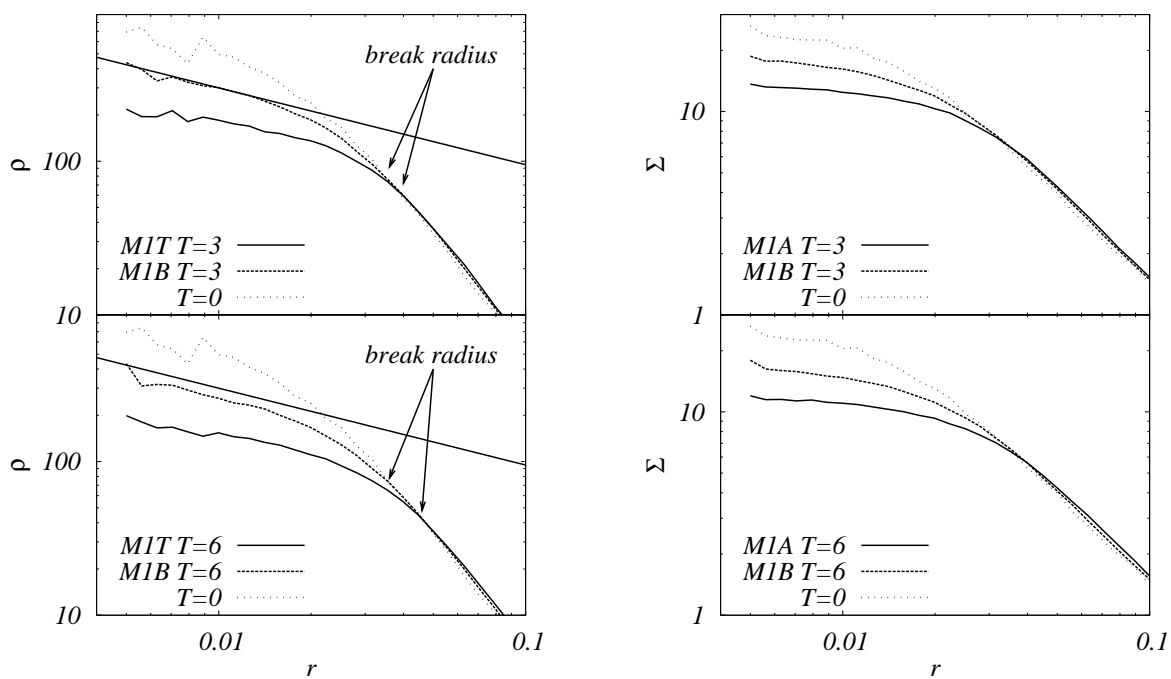


Fig. 2.— Volume (left) and surface (right) density profiles for models M1T (solid) and M1B (dashed). Dotted curves show the initial profile. Solid lines indicate the power law  $\rho \propto r^{-0.5}$ . Top panel shows the profiles at  $T = 3$ , and bottom shows those at  $T = 6$ .

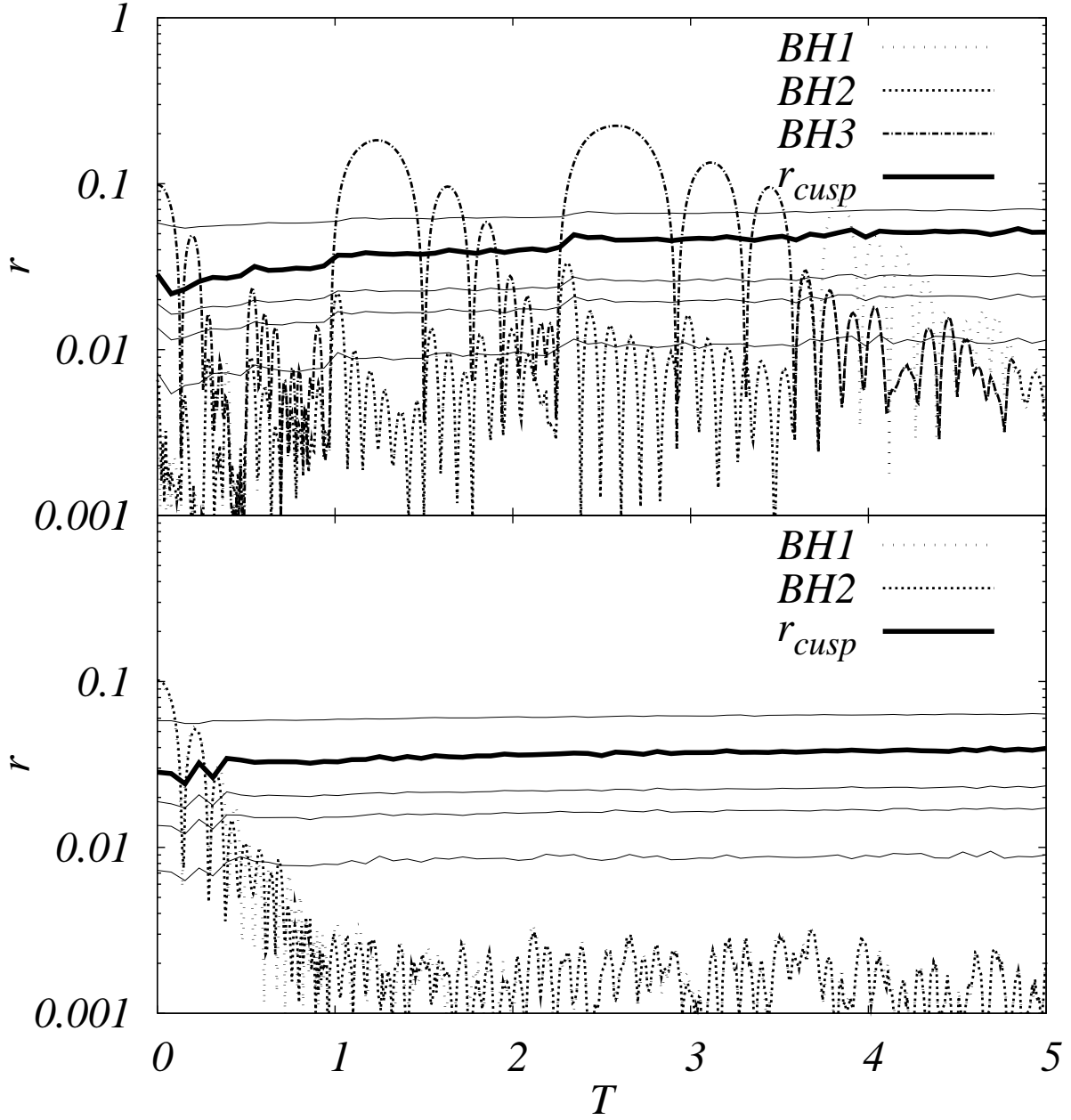


Fig. 3.— Evolution of Lagrangian radii, radial distance of BHs from the center of the galaxy, and the cusp radius, for models M1T(top panel) and M1B(bottom panel). The four solid curves show Lagrange radii (0.1%, 0.5%, 1%, 5% of total mass). Thick dashed, dotted and dash-dotted curves show the radial distances from the galactic center for BHs. Thick solid curves show the cusp radius.

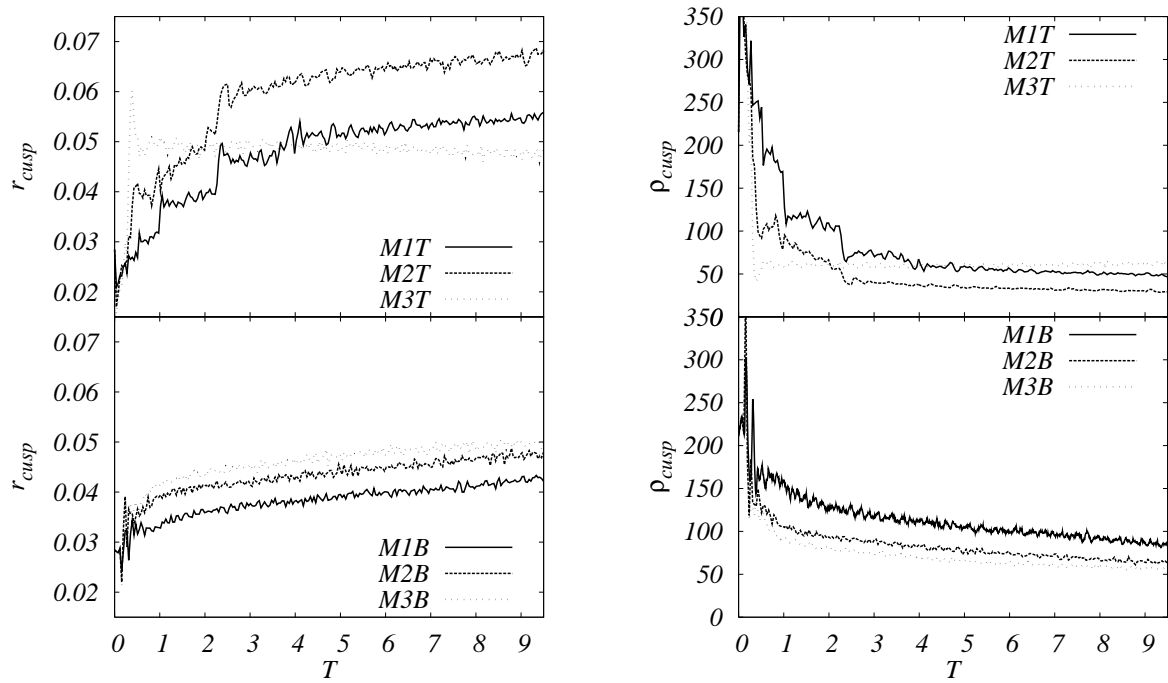


Fig. 4.— Evolution of cusp radii (left) and cusp densities (right) for all models. Top and bottom panels show the results for triple and two BH models respectively. Solid, dashed, and dotted curves represent the results of models M1x, M2x and M3x.



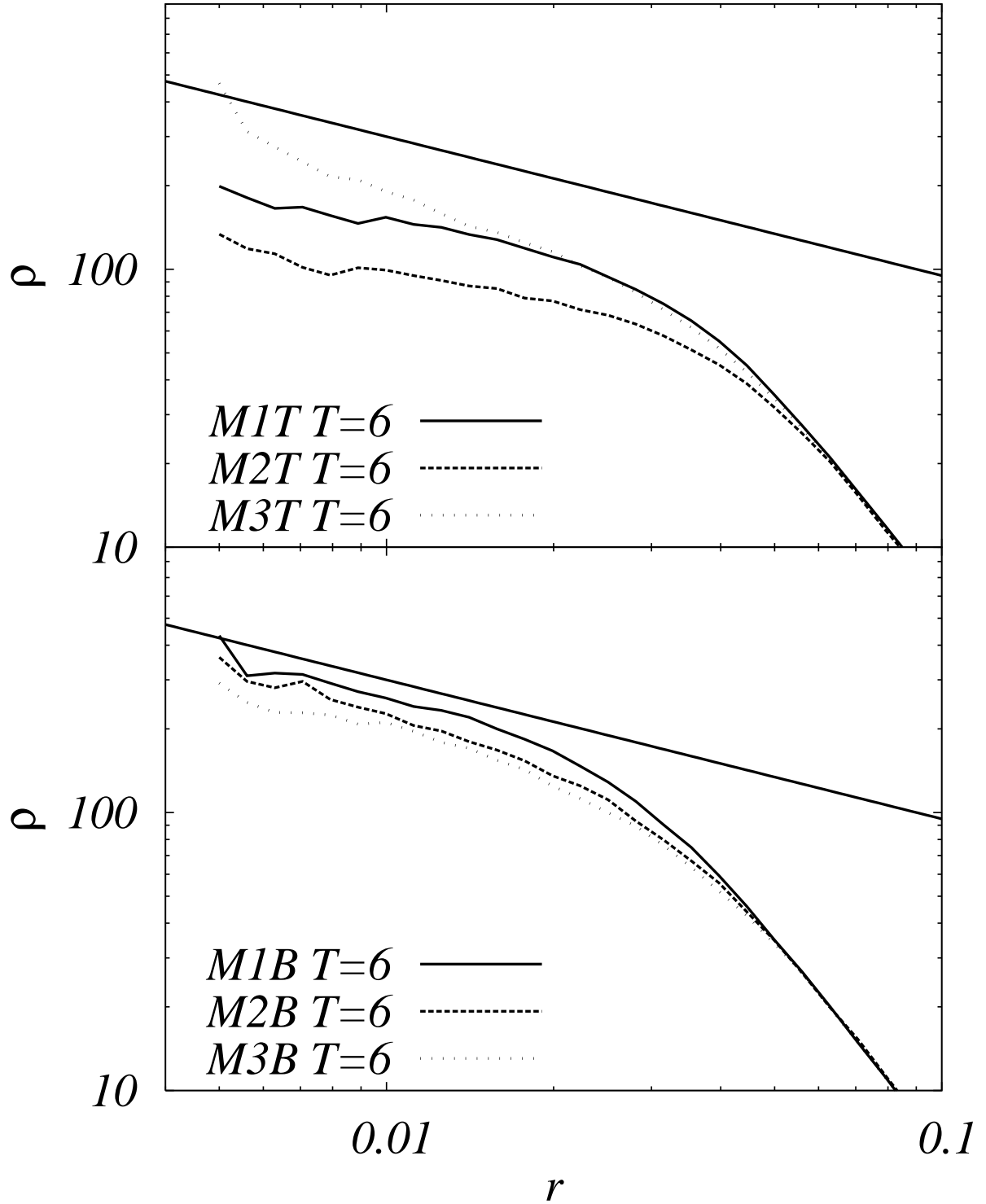


Fig. 5.— Spatial density profiles for all runs at  $T = 6$ . Solid lines indicate the power law  $\rho \propto r^{-0.5}$ . Top panel shows the results of three-BH models, and bottom shows those of two-BH models.

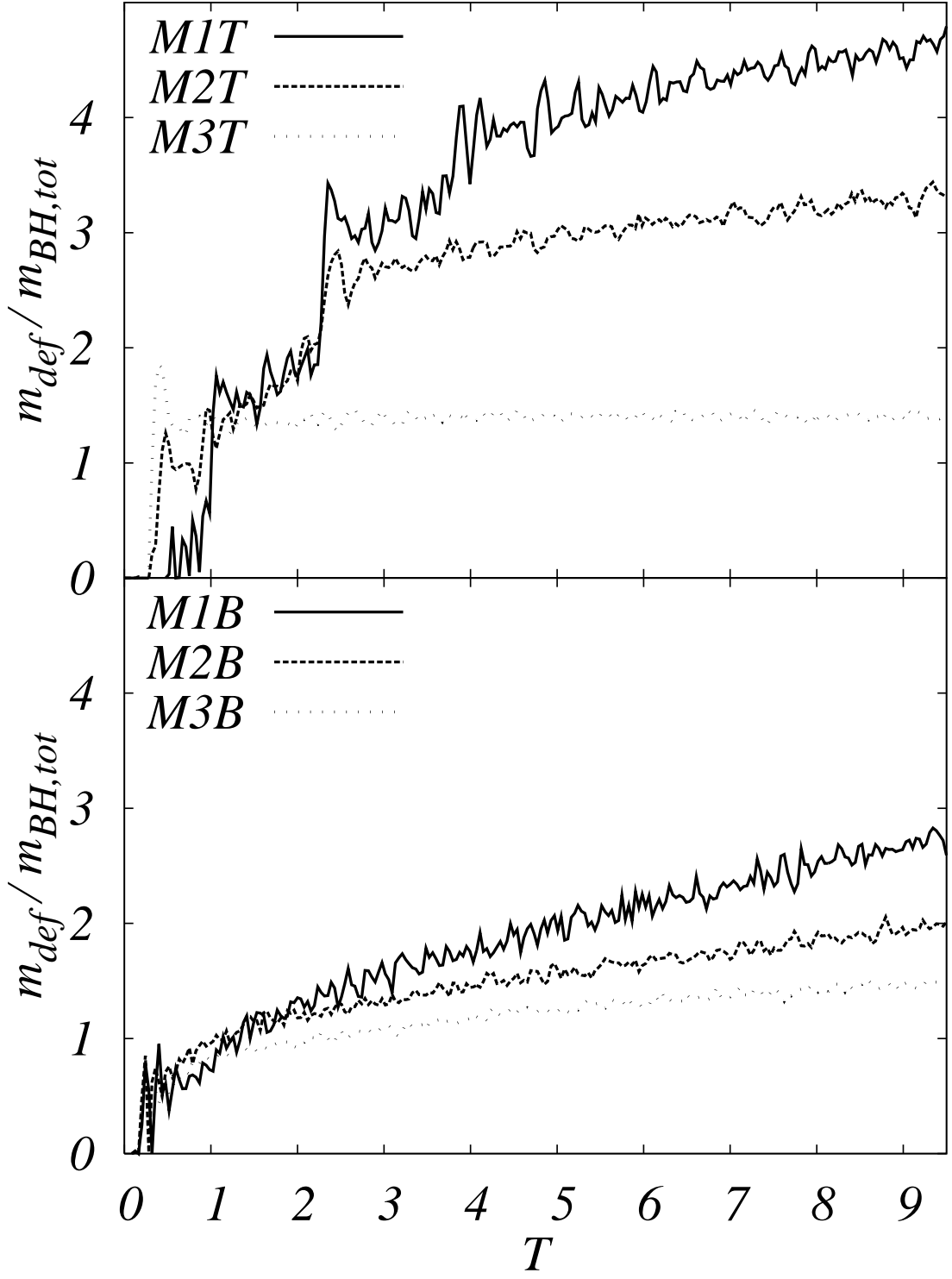


Fig. 6.— Time evolution of  $m_{def}$  normalized by  $m_{BH,tot}$  for all models. Top and bottom panel show the results of triple- and two-BH models respectively.

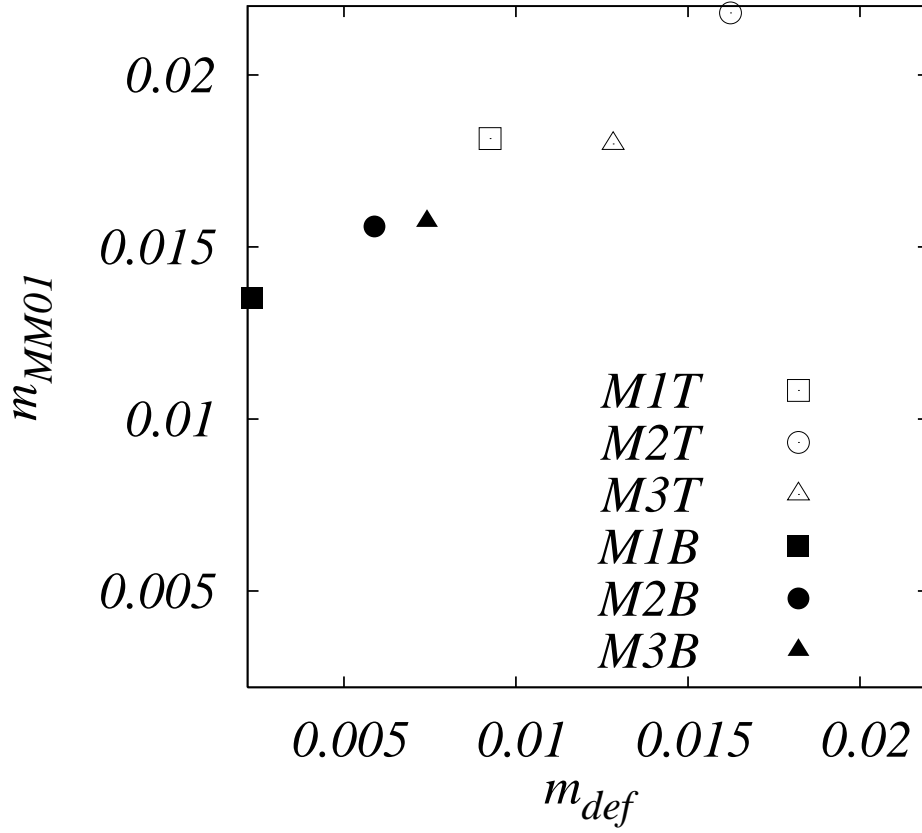


Fig. 7.— Mass deficit estimated with MM2001’s methods and the real value. For MxB runs,  $m_{def}$  is calculated at  $T = 1$ , and for MxT runs at  $T = 3$ .

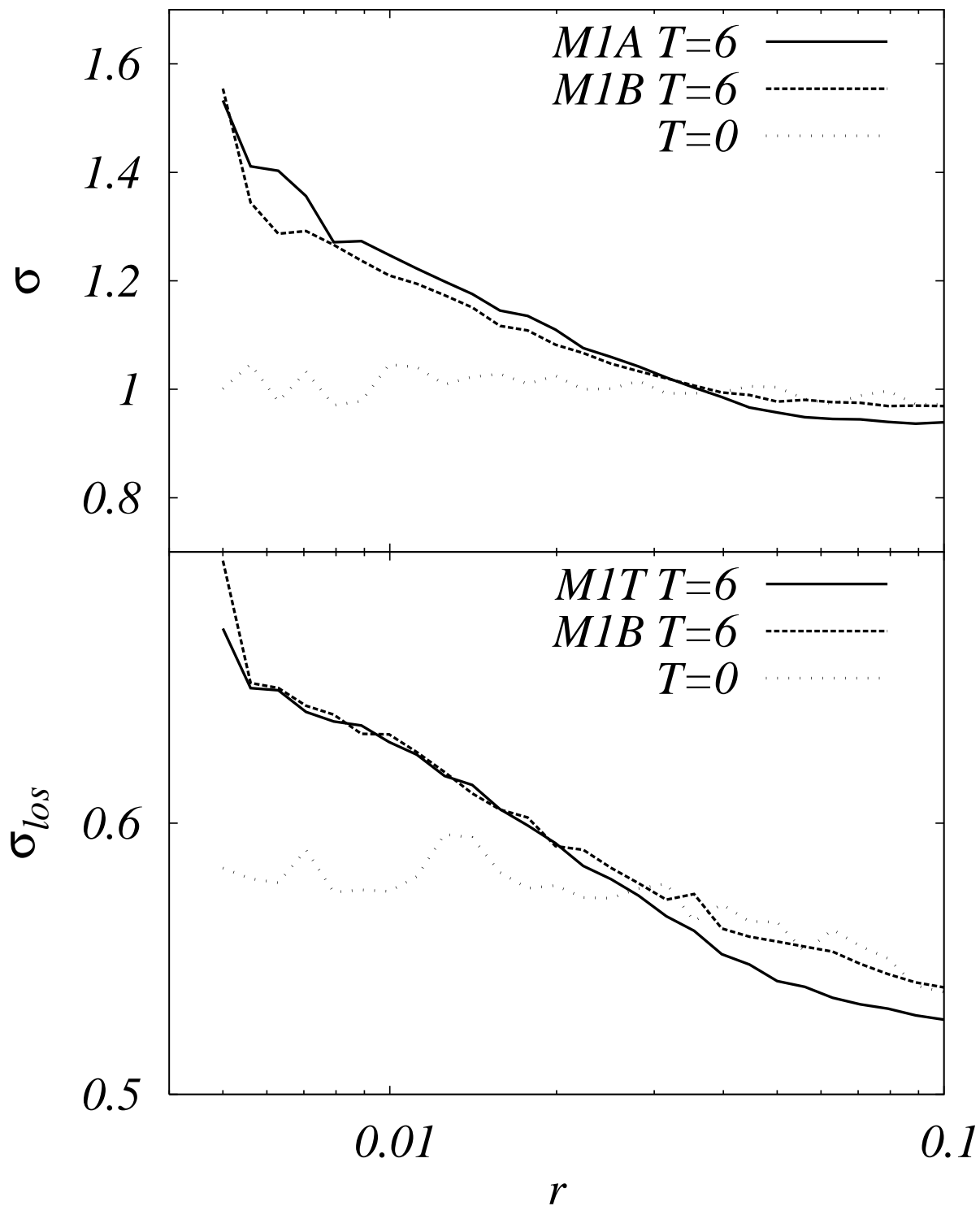


Fig. 8.— Velocity dispersion (top) and line-of-sight velocity (bottom) profiles at  $T = 6$  for models M1T and M1B. Solid and dashed curves show three- and two-BH cases respectively, and dotted curves show the initial profiles.

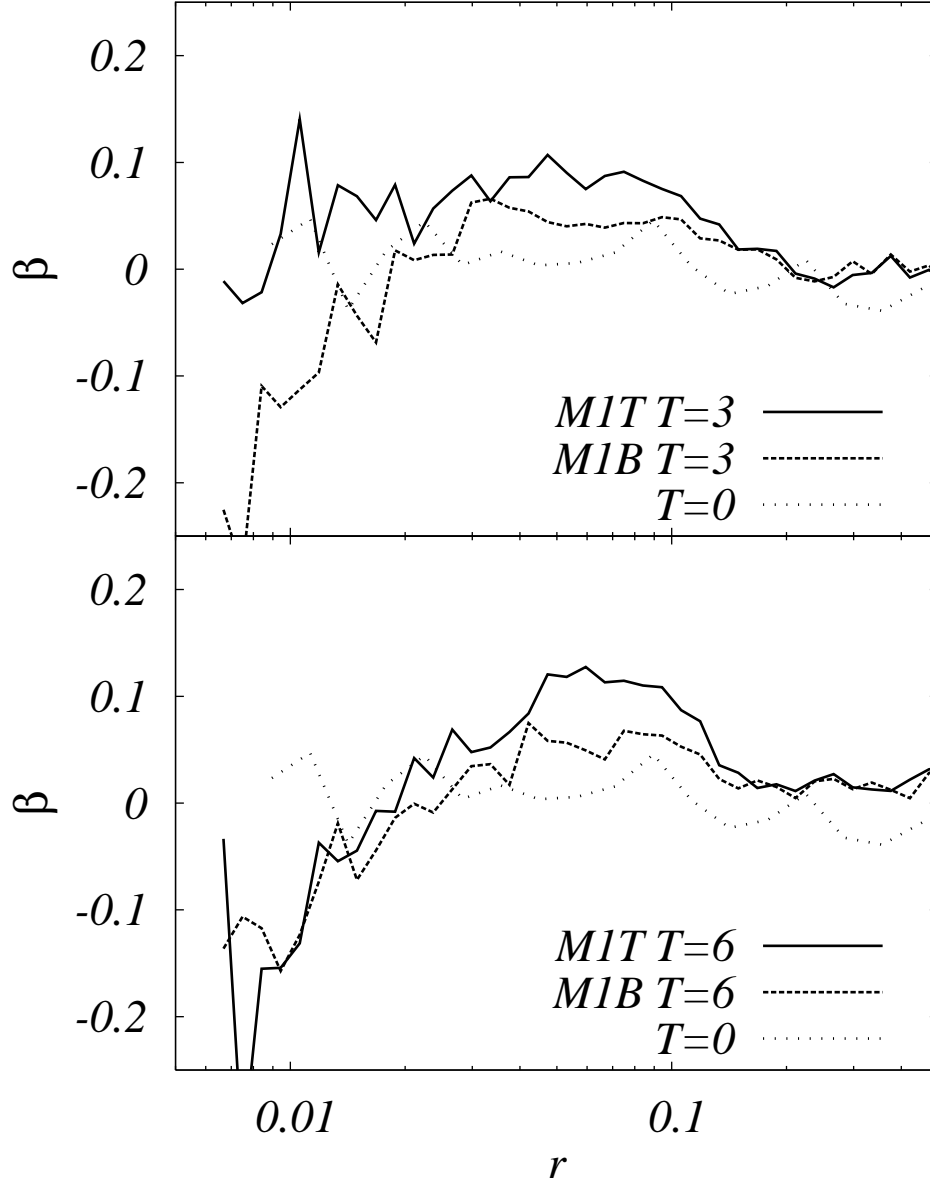


Fig. 9.— Anisotropy parameter for models M1T and M1B. Solid and dashed curves show the results of three- and two-BH cases respectively, and dotted curves show the initial profiles.